Electronic Supplementary Material (ESI) for Journal of Materials Chemistry A.

Supporting Information

Cooperative Template Strategy to Control Pore Structure of ZIF-Derived Carbon for Fuel Cell Cathode

Zhihong Huang, Mingjia Lu, Sucheng Liu, Longhai Zhang, Yangyang Chen, Lecheng Liang, Jiaxi Zhang, Huiyu Song, Li Du, and Zhiming Cui*

Guangdong Provincial Key Laboratory of Fuel Cell Technology, School of Chemistry and Chemical Engineering, South China University of Technology, Guangzhou 510641, China.

Corresponding Author:

*E-mail: zmcui@scut.edu.cn. (Prof. Zhiming Cui)

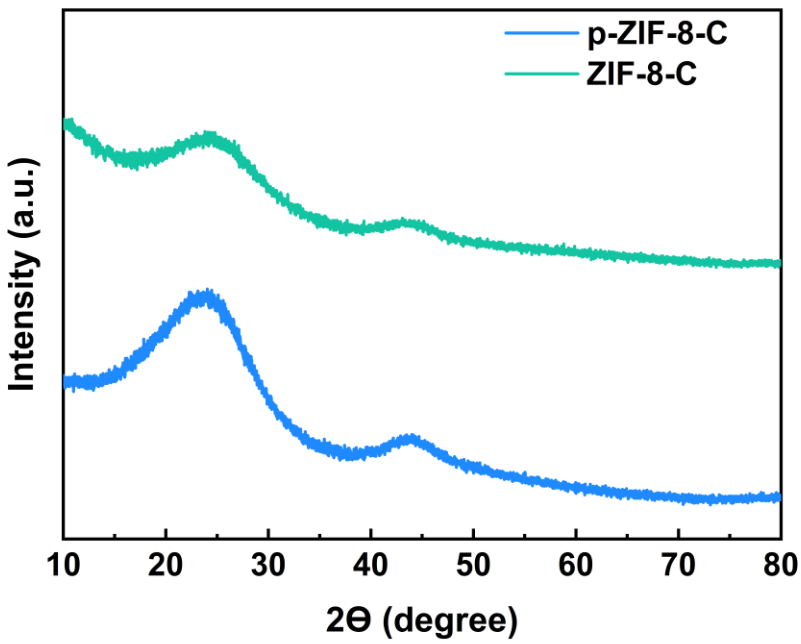

Fig. S1. XRD patterns of p-ZIF-8-C and ZIF-8-C.

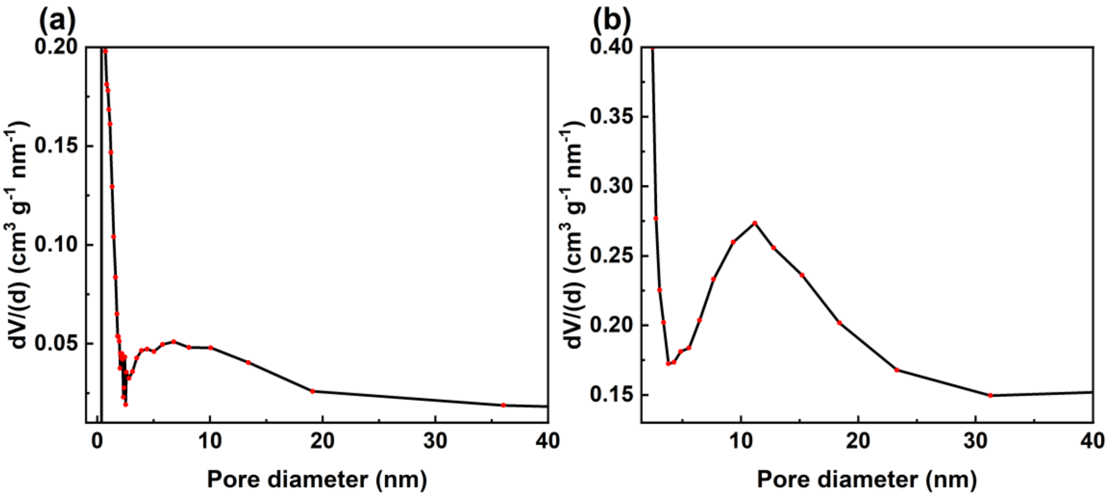

Fig. S2. Pore size distributions for p-ZIF-8-C with different molar amounts of SL (a) 2 mmol, (b) 5 mmol.

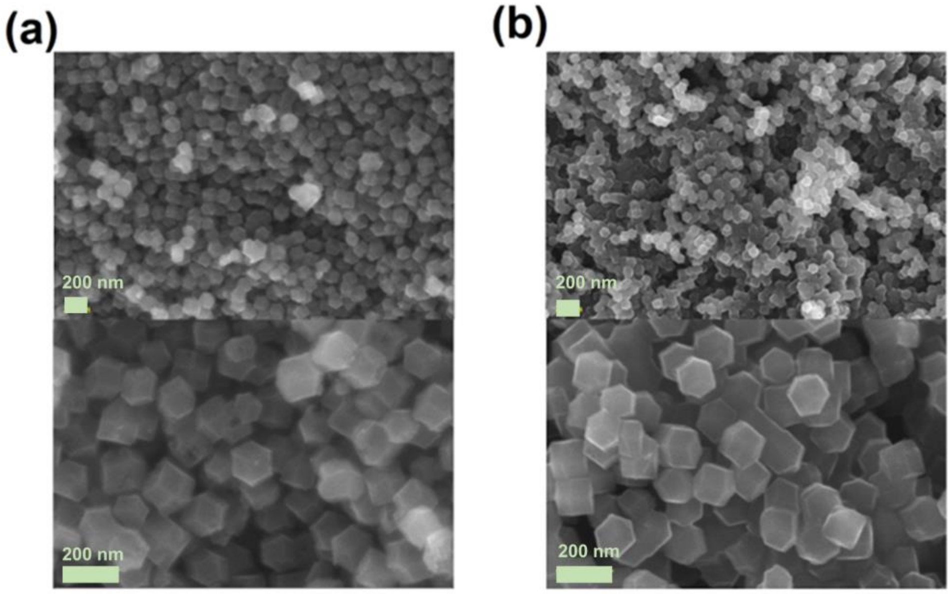

Fig. S3. SEM images of (a) p-ZIF-8-C and (b) ZIF-8-C.

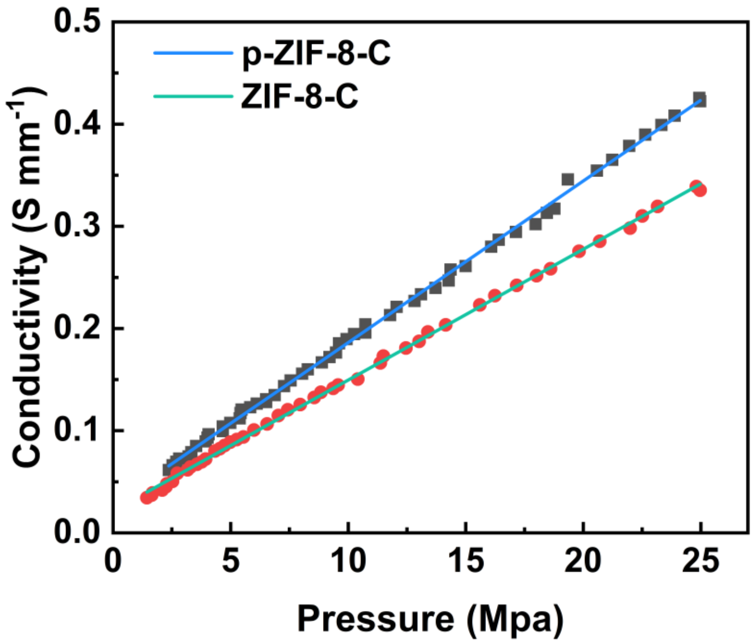

Fig. S4. Conductivity diagram of p-ZIF-8-C and ZIF-8-C.

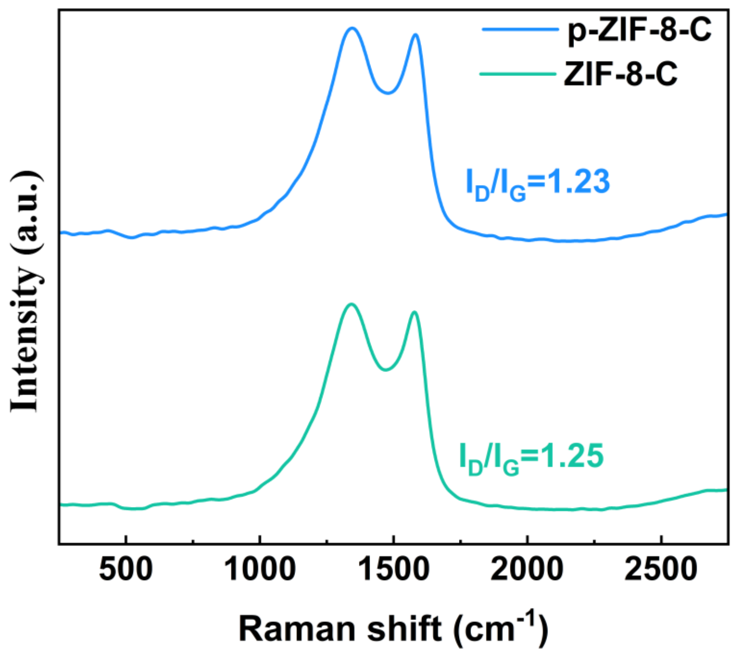

Fig. S5. Raman spectras of p-ZIF-8-C and ZIF-8-C.

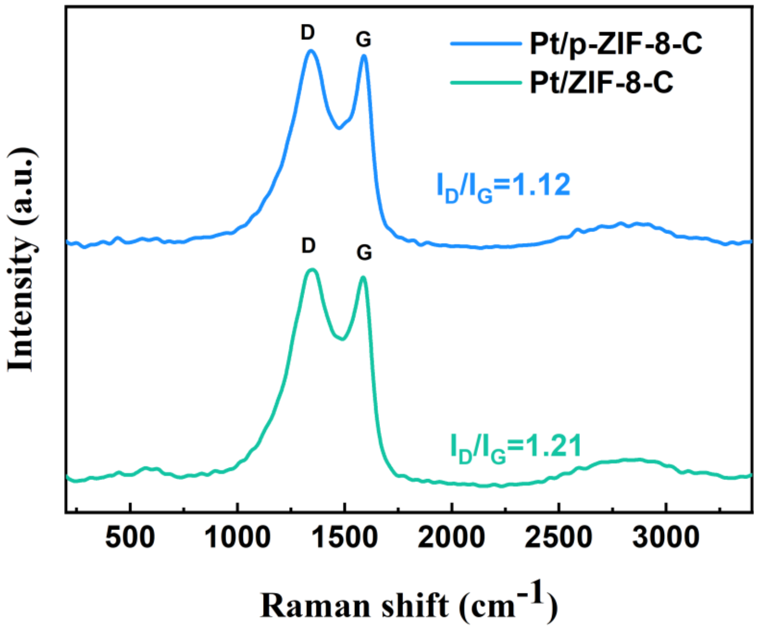

Fig. S6. Raman spectras of Pt/p-ZIF-8-C and Pt/ZIF-8-C.

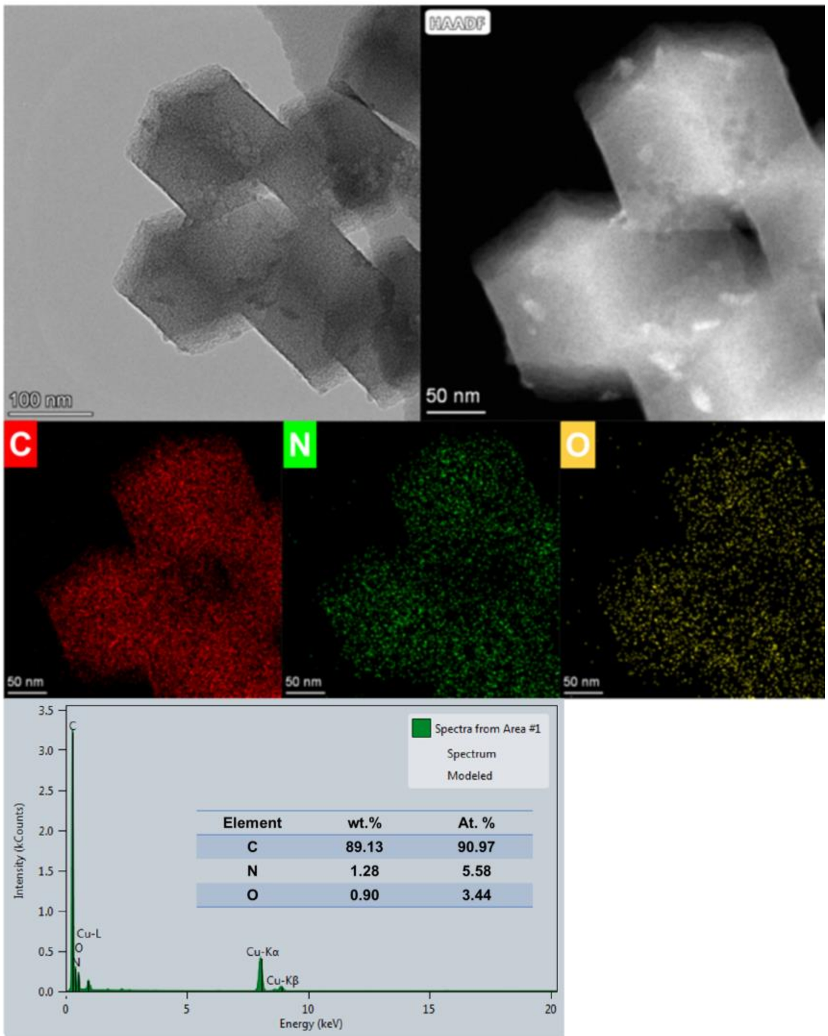

Fig. S7. HAADF-STEM image, elemental mappings of p-ZIF-8-C and the spectra along with wt.% and At.% of C, N and O in p-ZIF-8-C.

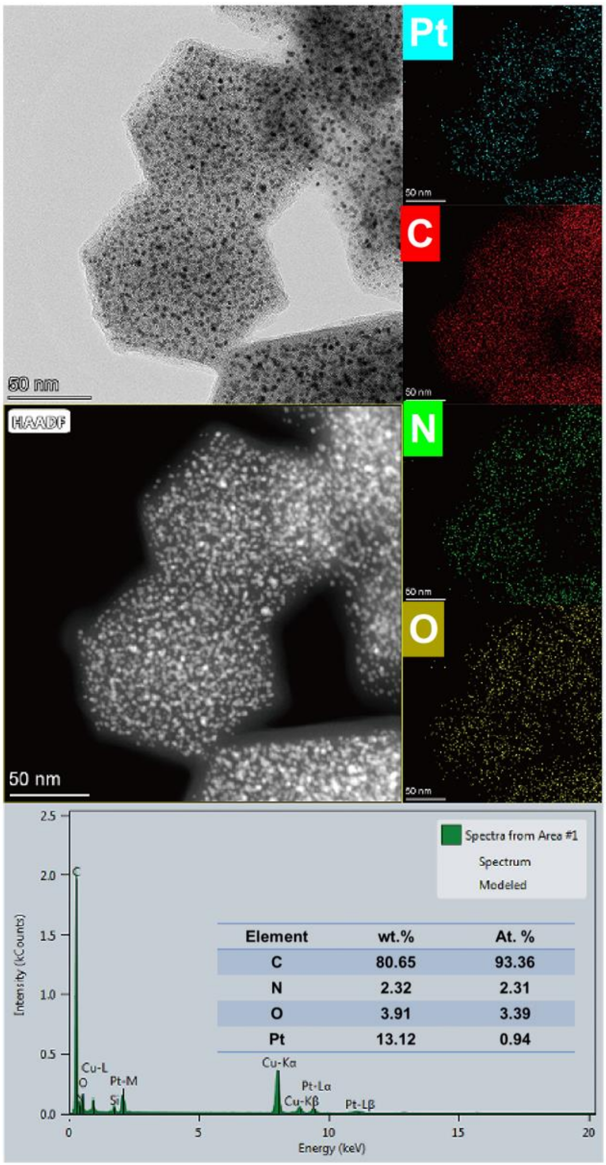

Fig. S8. HAADF-STEM image, elemental mappings of Pt/ZIF-8-C and the spectra along with wt.% and At.% of Pt, C, N and O in Pt/ZIF-8-C.

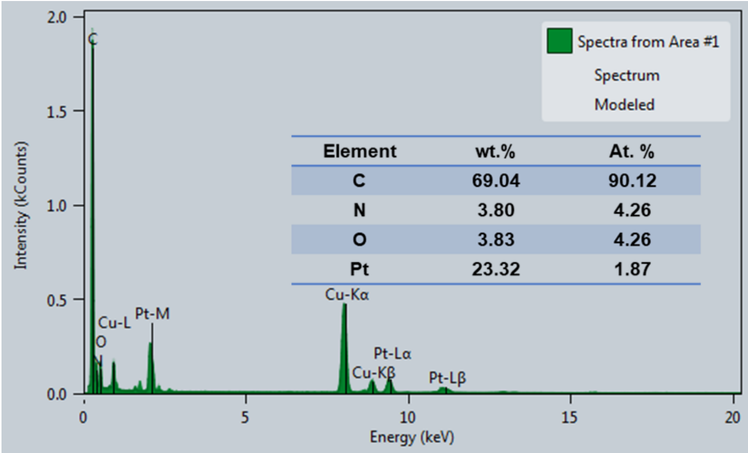

Fig. S9. The spectra along with wt.% and At.% of Pt, C, N and O in Pt/p-ZIF-8-C.

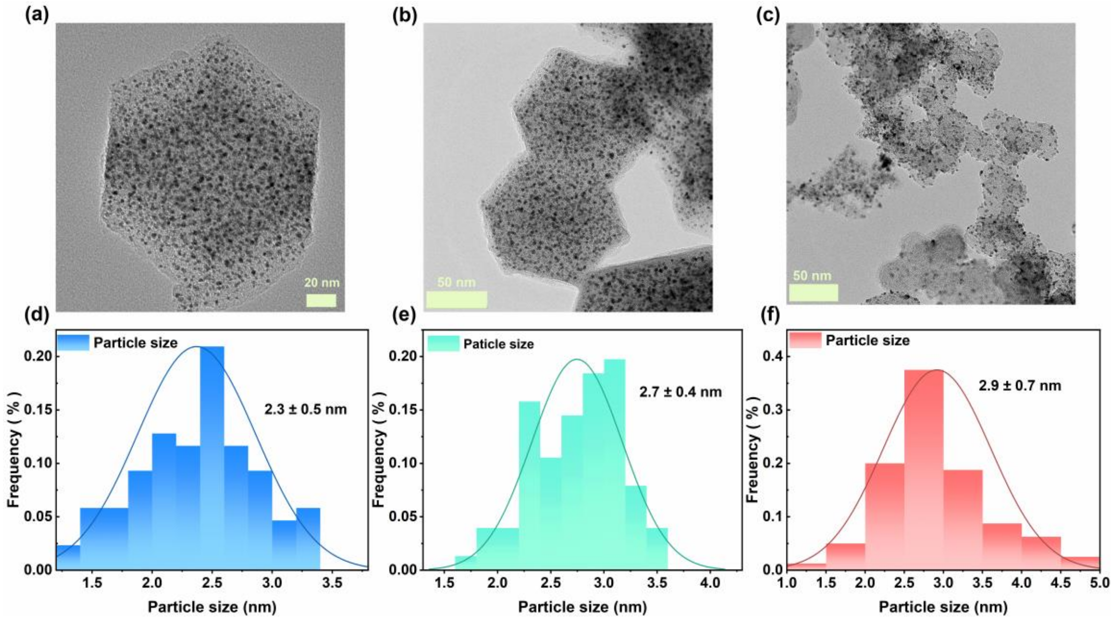

Fig. S10. TEM images and histograms of (a, d) Pt/p-ZIF-8-C, (b, e) Pt/ZIF-8-C, (c, f) JM 20wt.% Pt/C.

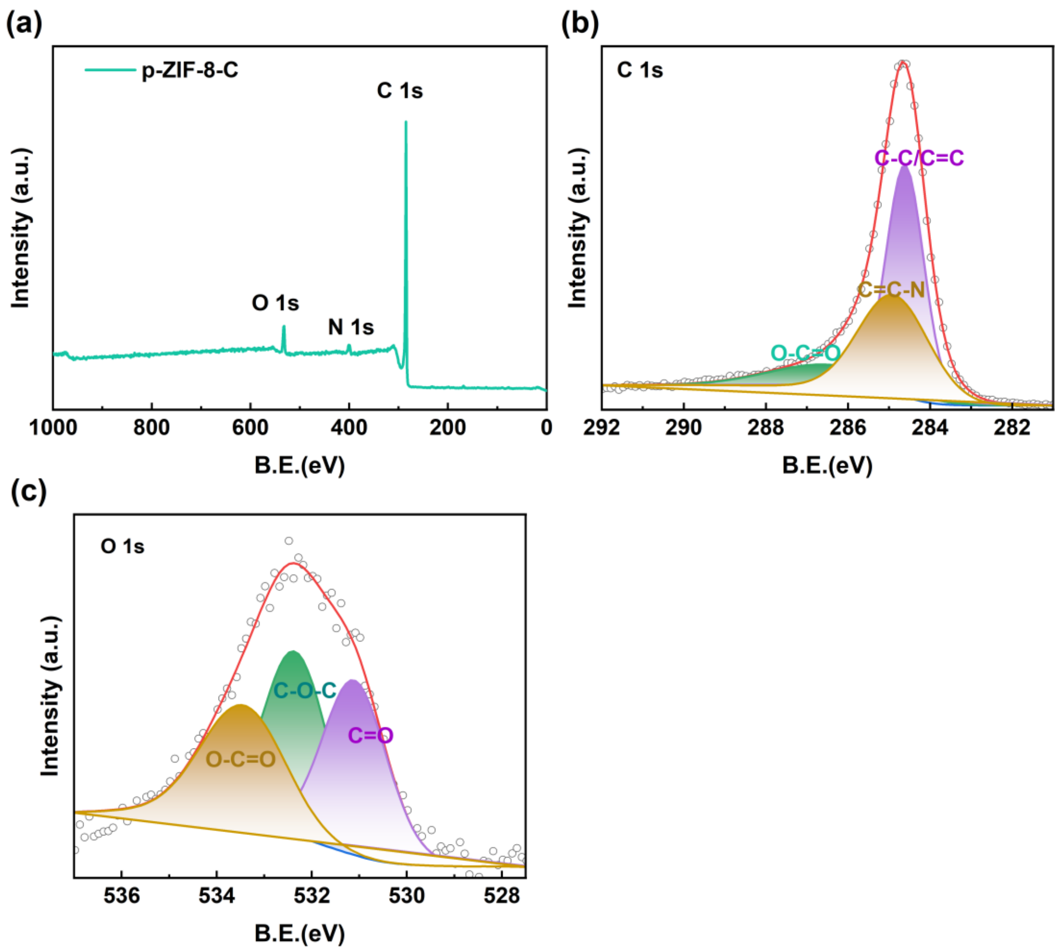

Fig. S11. (a) Survey XPS spectra, (b-c) C 1s and O1s of p-ZIF-8-C.

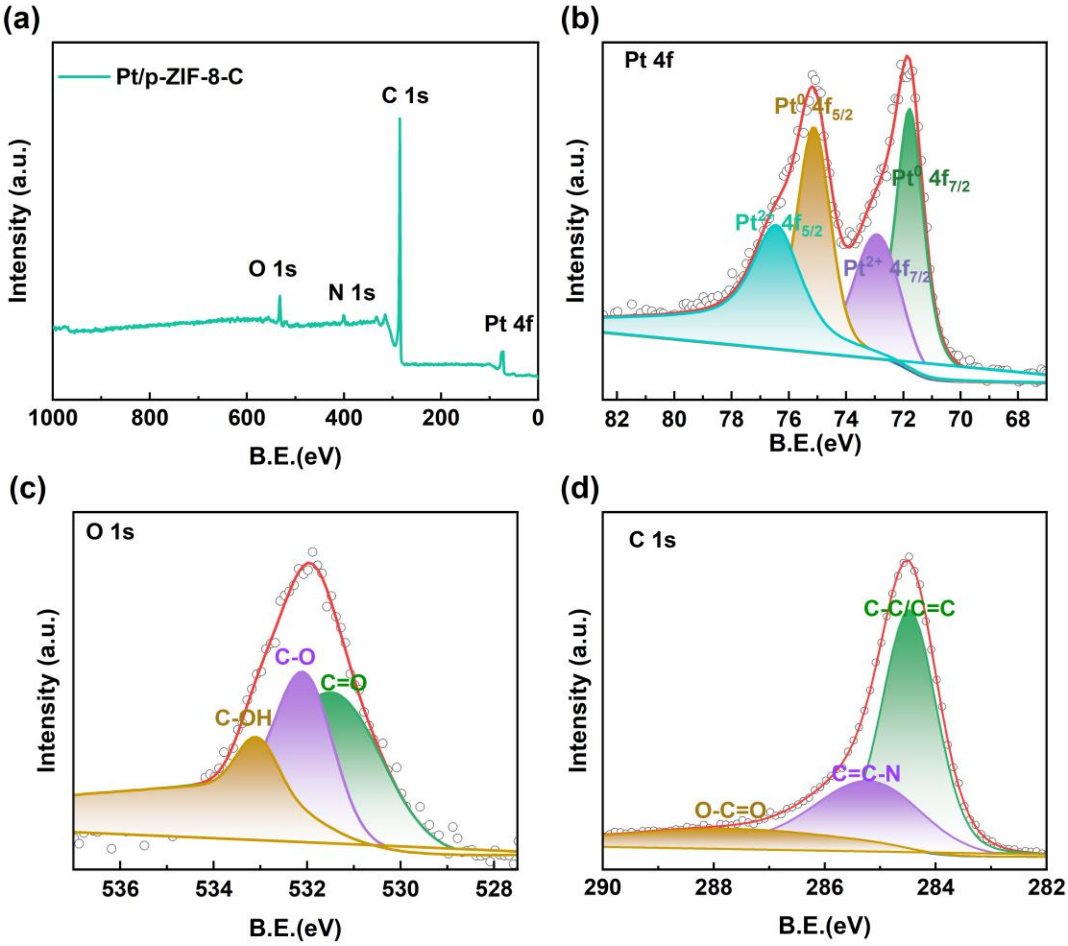

Fig. S12. (a) Survey XPS spectra, (b-d) Pt 4f, O 1s and C1s of Pt/p-ZIF-8-C.

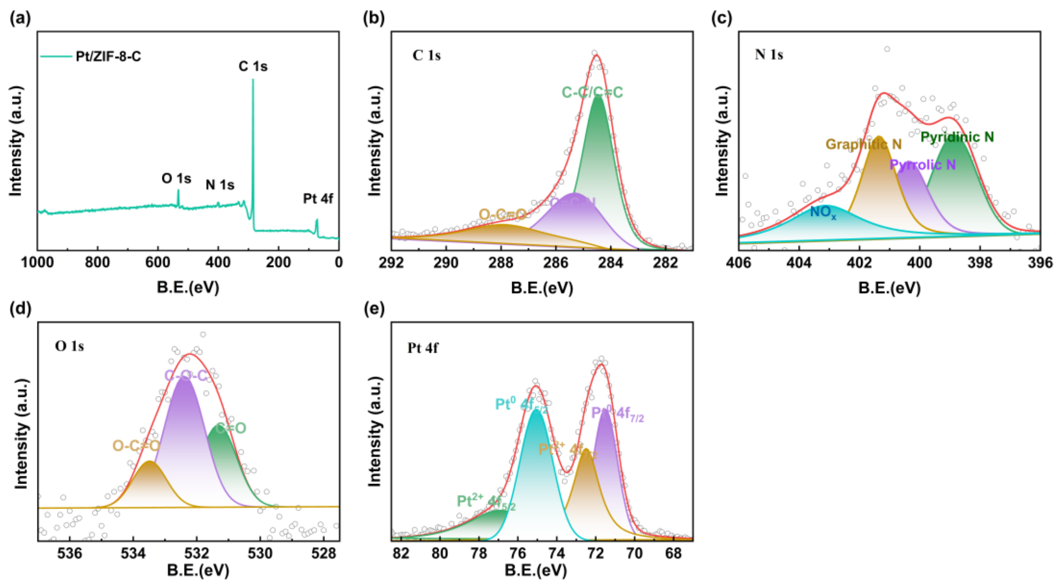

Fig. S13. (a) Survey XPS spectra, (b-e) C 1s, N 1s, O 1s and Pt 4f of Pt/ZIF-8-C.

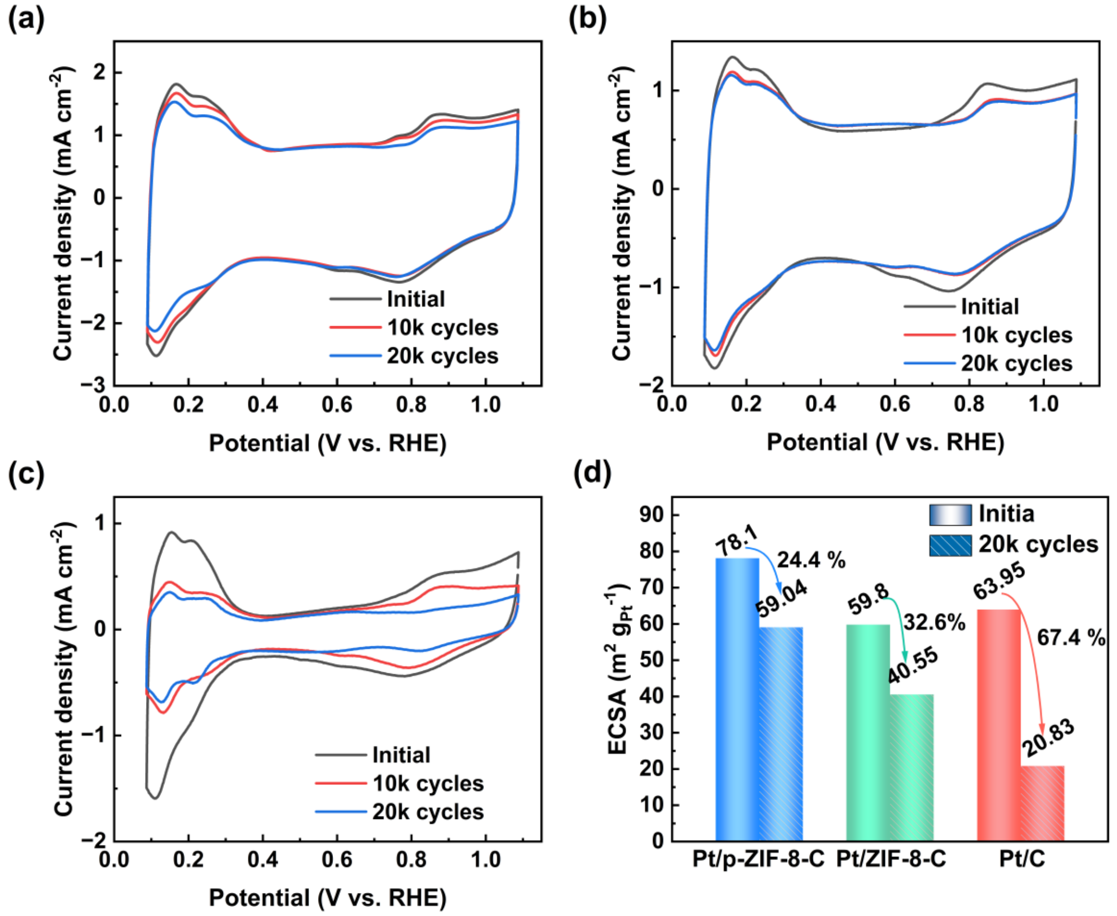

Fig. S14. (a-c) The CVs; (d) ECSA of Pt/p-ZIF-8-C, Pt/ZIF-8-C and JM 20wt.% Pt/C before and after 20k ADT.

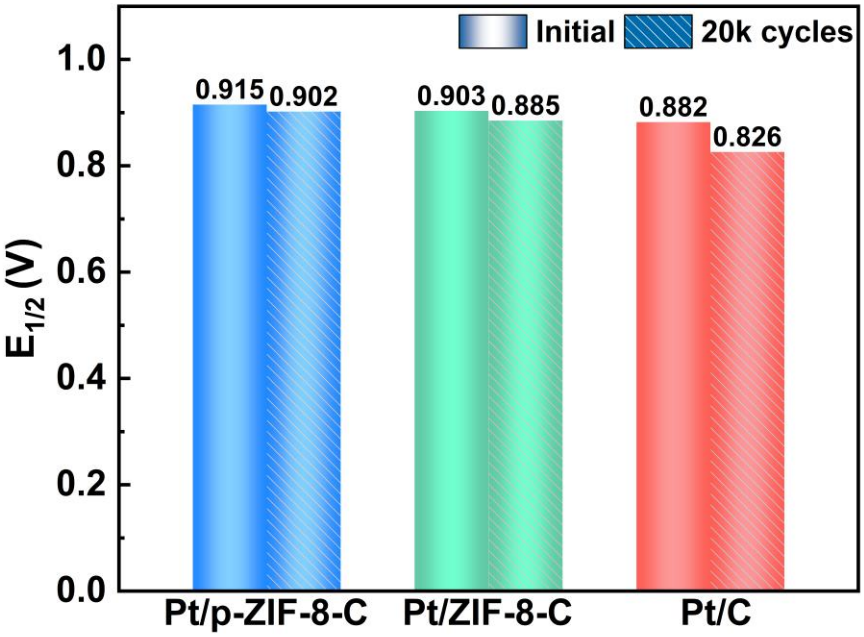

Fig. S15. The $E_{1/2}$ of Pt/p-ZIF-8-C, Pt/ZIF-8-C and JM 20 wt.% Pt/C before and after 20k ADT.

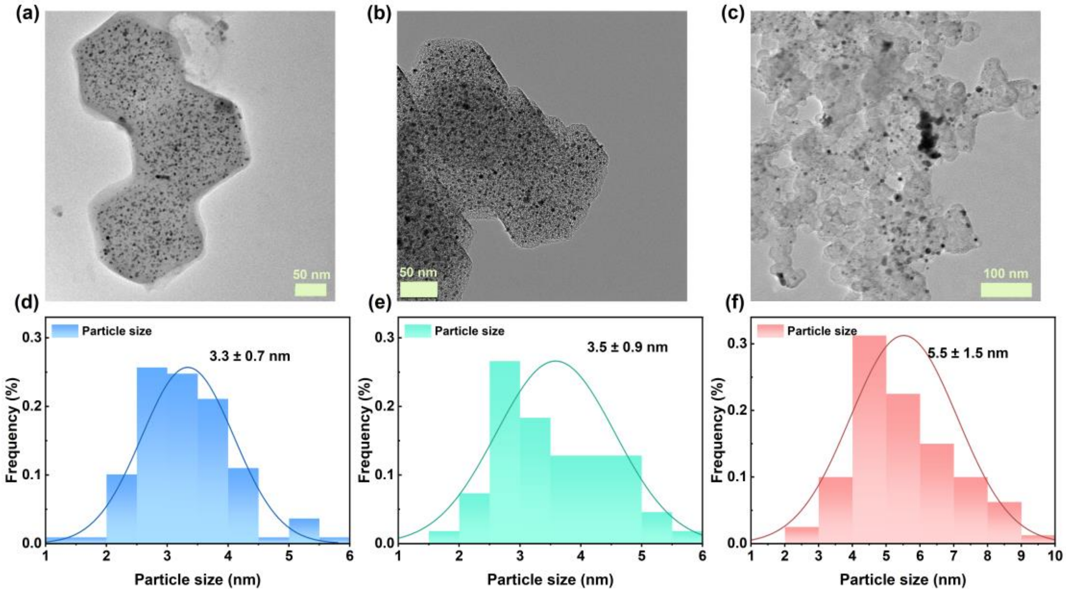

Fig. S16. TEM images and histograms of (a, d) Pt/p-ZIF-8-C, (b, e) Pt/ZIF-8-C, (c, f) JM 20 wt.% Pt/C after 20k ADT.

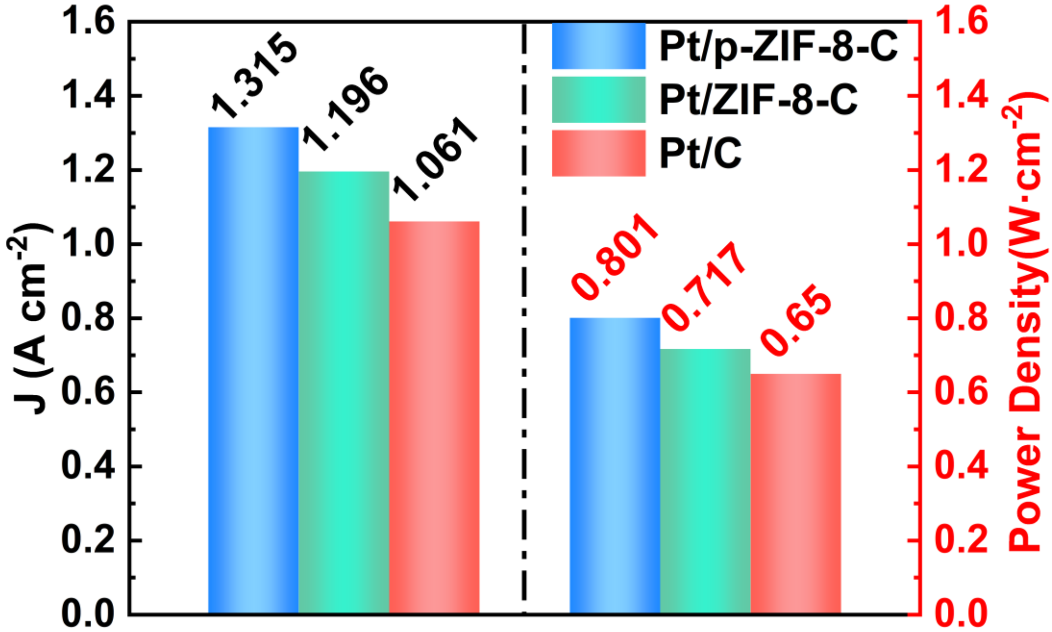

Fig. S17. histogram of current density at 0.6V and maximum power density of Pt/p-ZIF-8-C, Pt/ZIF-8-C and JM 20 wt.% Pt/C as the cathode.

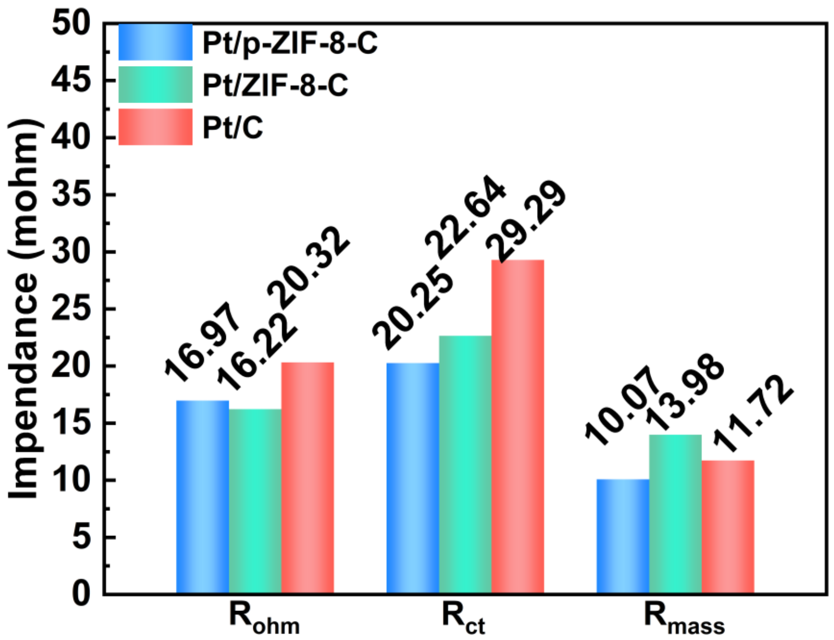

Fig. S18. Impedance of each part for Pt/p-ZIF-8-C, Pt/ZIF-8-C and 20 wt.% Pt/C measured at 800 mA cm^{-2} under 100% RH.

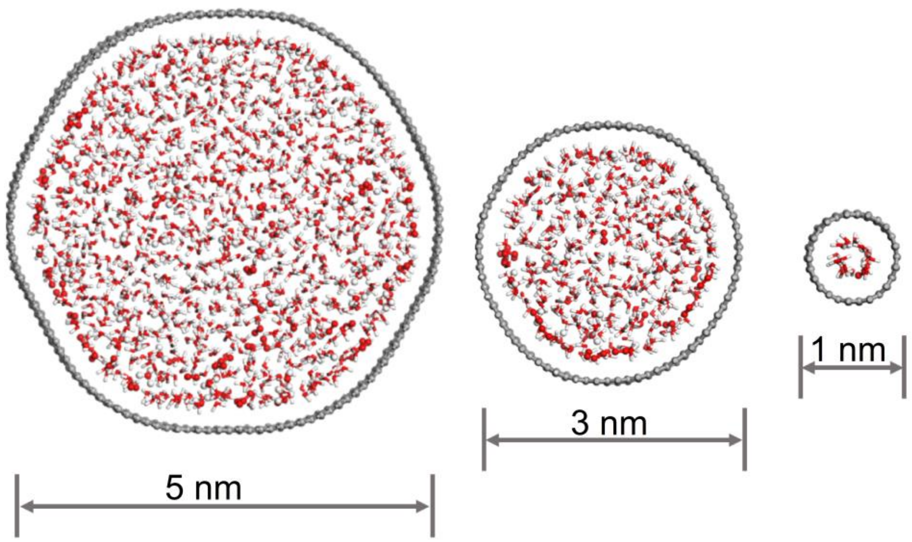

Fig. S19. Structure models of different pores for MD simulation.

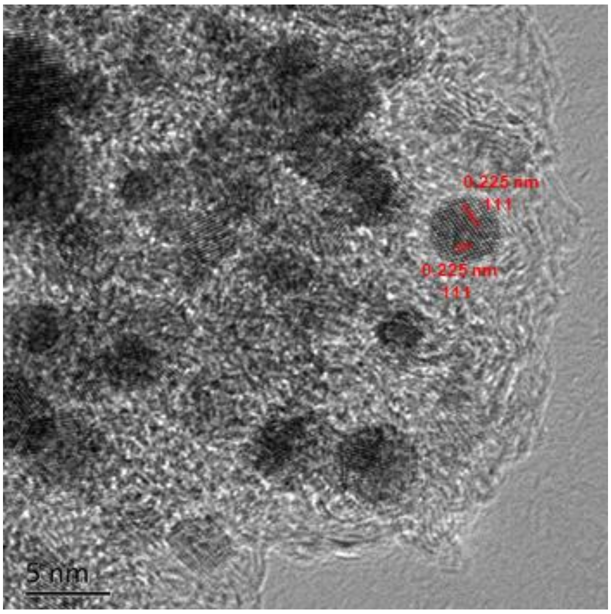

Figure S20. HR-TEM image of Pt NPs;

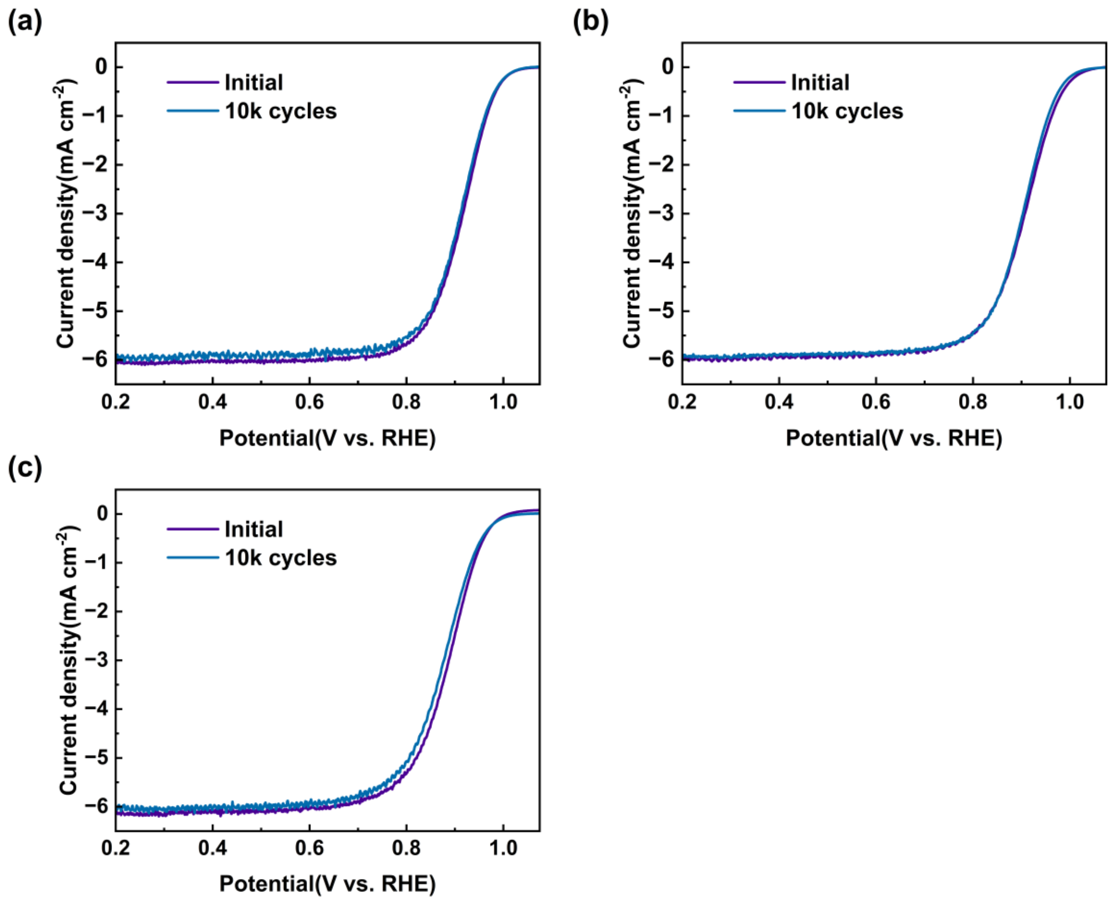

Fig. S21. LSV curves of (a) Pt/p-ZIF-8-C, (b)Pt/ZIF-8-C and (c) JM 20.wt% Pt/C after AST test under a high potential range (1.0–1.5 V).

Table S1. Performance comparisons of different ORR catalysts in RDE.

Catalyst	$E_{1/2}$ / V vs RHE	Mass activity （A mg_{pt}^{-1}）	Ref.
Pt/p-ZIF-8-C	**0.915**	**0.44**	**This work**
Pt/ZIF-8-C	**0.903**	**0.32**	
Pt–Nb_2O_5	—	0.220	*ACS Catal.* **2022,** 12, 13523-13532.
40% Pt–$Co_6Mo_6C_2$/^{g}C	0.92	0.271	*J. Am. Chem.Soc.* **2012,** 13, 1954-1957.
Pt/ALDTa_2O_5/C	0.891	0.222	*Nano Energy* **2018,** 53, 716-725.
Pt/N-ALDTa_2O_5/C	0.908	0.280	
Pt/N,P-CNTs	0.91	0.285	*Electrochim. Acta* **2015,** 158, 374-382.
Pt/N-CNTs	0.87	0.165	
Pt/SG (sulfur-doped -graphene)	—	0.139	*Adv. Funct. Mater.* **2014,** 24, 4325-4336.
Pt/G (graphene)	—	0.101	
Pt-SA/NCx	0.935	0.58	*Adv. Funct. Mater.* **2023,** 33 , 2302582.
Pt/OMC–CNT	—	0.232	*J. Mater. Chem. A* **2013,** 1, 1270-1283
Pt/cPDA	—	0.94	*Nat. Commun.* **2022,** 13, 6157.